23.0 Plasma Dynamics

Academic and Research Staff

Prof. G. Bekefi, Prof. A. Bers, A. Ram, Prof. B. Coppi

Visiting Scientists

V. Fuchs[1], C. Lashmore-Davies[2]

Graduate Students

K. Kupfer

23.1 Relativistic Electron Beams

U.S. Air Force - Office of Scientific Research (Grant AFOSR 84-0026)
National Science Foundation (Grant ECS 85-14517)
U.S. Department of Energy (Contract DE-FG05-84ER 13272)
Lawrence Livermore National Laboratory (Subcontract 6264005)

George Bekefi

During the past year we have undertaken four studies: 1) nonlinear characteristics of the free electron laser; 2) measurements of electron temperature on the free electron laser gain; 3) optical guiding measurements; and 4) the design of a new type of helical wiggler.

23.1.1 Nonlinear Characteristics of the Free Electron Laser

We have completed measurements of the nonlinear radiation intensity and of the wave refraction index of our free electron laser. This laser operates in the Raman regime. Power saturation, synchrotron oscillations, and the wave refractive index were studied as a function of beam energy, beam current and the axial position within the wiggler. Very good agreement with computer simulations have been obtained.

23.1.2 Effect of Electron Beam Temperature on FEL Operation

At sufficiently low beam currents, electron beam temperature effects cause the gains of collective (Raman) regime free electron lasers to be lower than the predictions of cold beam theory. This gain degradation has been measured as a function of the beam current, the wiggler magnetic field and the interaction frequency. The measurements are used to estimate the electron beam temperature, and the estimated temperature is close to the temperature predicted by numeric simulations.

---

1 Visiting Scientist, I.R.E.Q., Quebec, Canada

2 Visiting Scientist, Culham Laboratory, U.K.A.E.A., Abingdon, Oxfordshire, England

23.1.3 Optical Guiding Measurements

Optical guiding is an important phenomenon predicted by theory, but as yet not observed experimentally. This phenomenon would mitigate the effects of diffraction and thereby allow the length of FEL wigglers to exceed the Rayleigh range. We carried out what we believe are the first measurements of optical guiding.

23.1.4 The Design of a New Type of Helical Wiggler

We have come up with a very simple design for a permanent magnet helical wiggler which may be useful for free electron laser and cyclotron maser applications. The wiggler is composed of a cyclindrical array of staggered samarian-cobalt bar magnets.

During the coming year we plan to continue work in all areas described above. In addition, we will undertake an experimental and theoretical study if free electron efficiency enhancement. To this purpose, we have designed a helical wiggler in which the periodicity is tapered to allow the electrons to remain in phase synchronism with the wiggler field.

23.2 Plasma Wave Interactions - RF Heating and Current Generation

National Science Foundation (Grant ECS 82-13430)
U.S. Department of Energy (Contract DE-AC02-78-ET-51013)

Abraham Bers, Vladimir Fuchs, Chris Lashmore-Davies, Abhay Ram, Kenneth Kupfer

Our analytical and computational work of the past year is briefly described in the following four subsections. A general theoretical framework was developed for treating mode-conversion and instability in inhomogeneous plasmas (subsection 23.3). This has lead to a new formulation of the transmission coefficient through the mode-conversion region of a fast-Alfven wave with an ion-Bernstein wave (subsection 23.4.1). Analytic description of the ion-Bernstein wave parallel-wavenumber enhancement due to toroidal effects have been obtained (subsection 23.4.2). Studies of lower-hybrid current drive have continued to address and evaluate relativistic effects (subsection 23.5). We have also extended the formulation and identification of absolute instabilities from dispersion relations that are transcendental in the wavenumber (subsection 23.6); this has proven useful in identifying the onset of von-Karman vortices in fluid dynamics as a transition from convective to absolute instability.

23.3 Coupled-Mode Propagation and Instability in Inhomogeneous Plasmas

The free energy of a plasma system is often associated with the distribution of particles in velocity space (e.g., anisotropic temperature, drifts, etc.). Linear theory exhibits this free energy in the form of stable negative-energy waves. These waves are driven unstable when coupled to positive-energy waves, or when positive dissipation extracts free energy from the system. The space-time evolution of such instabilities is well un-

derstood for the case of infinite, homogeneous plasmas; yet in many real systems, which are inherently finite and nonuniform, it is the very presence of the spatial inhomogeneity which allows the unstable coupling to take place. A general theoretical framework has been developed to treat such linear coupled-mode instabilities in weakly nonuniform plasmas.[1] We have developed two independent, yet supporting, formalisms that allow for the extraction of an embedded pairwise coupling event from a general local dispersion relation, and provide an unambiguous partial differential equation, second order in both space and time, describing the space-time evolution of the resulting instability.

The first approach requires the expansion of the local dispersion relation, $D(k_x, \omega; x) = 0$, about special mode boundaries in Fourier-Laplace transform space. This generalizes our earlier work on propagation and mode conversion in stable plasmas.[2] The mode boundaries isolate the various branches of the local dispersion relation, and allow for analytic continuation of the modes only at the appropriate coupling points, k_{x0}, ω_0 , and x_0, given by the three (generally complex) conditions:

$$D(k_{x0}, \omega_0; x_0) = 0, \tag{1}$$

$$\frac{\partial D}{\partial k_x}\bigg|_0 = 0, \tag{2}$$

and

$$\frac{\partial D}{\partial \omega}\bigg|_0 = 0. \tag{3}$$

In general, such coupling points will be six-dimensional objects, and represent branch points in the complex x -plane, and saddle points in both the complex k_x-plane and the complex ω-plane. This means that for a frequency fixed at the coupling point frequency, ω_0, two branches of the mapping:

$$D(k_x, \omega_0;\ x) = 0;\ x \in C, k_x = f_k(C) \tag{4}$$

will meet at k_{x0}, provided that the contour C passes through x_0 . Likewise, for a wavenumber fixed at $k_x = k_{x0}$ two branches of the mapping:

$$D(k_{x0}, \omega;\ x) = 0;\ x \in C, \omega = f_\omega(C) \tag{5}$$

will meet at ω_0 provided C passes through x_0. The modes are coupled both in space and time.

We require a boundary in the complex k_x -plane which confines the separate branches of the mapping in Eq.(4) to mutually exclusive regions of the complex k_x -plane. The branches are only allowed to intersect the mode boundary (and couple to other branches) at the coupling points, defined by Eqs. (1)-(3). At the same time, we require a boundary in the complex ω-plane which confines the different branches of the mapping in Eq.(5), and allows them to couple only at the coupling points. The two

boundaries which satisfy these conditions are found by simultaneously mapping the dependent contours:

$$\frac{\partial D(k_c(x), \omega_c(x);\ x)}{\partial k_x} = 0;\ x \in C, k_c(x) = g_k(C) \tag{6}$$

and

$$\frac{\partial D(k_c(x), \omega_c(x);\ x)}{\partial \omega} = 0;\ x \in C,\quad omega_c(x) = g_\omega(C) \tag{7}$$

With the mode boundaries so defined we are assured that the boundary $k_c = g_k(C)$ and the modes $k = f_k(C)$ have only the coupling wavenumber k_{x0} in common for $\omega = \omega_0$ The inverse mapping of $k_c = g_k(C)$ through the dispersion relation may therefore be interpreted as the appropriate branch cut in the complex x -plane:

$$C_{bk} = f_k^{-1}[g_k(C)]. \tag{8}$$

Likewise, for $k_x = k_{x0}$, we are assured that the boundary $\omega_c = g_\omega(C)$ and the modes $\omega = f_\omega(C)$ have only the coupling frequency ω_0 in common. The contour $\omega_c = g_\omega(C)$ therefore defines the boundaries of the Riemann sheets of the mapping $\omega = f_\omega(C)$, and the branch cut in the complex x-plane is given by:

$$C_{b\omega} = f_\omega^{-1}[g_\omega(C)]. \tag{9}$$

A pairwise space-time coupling event may be extracted from a general local dispersion relation by expanding to second order about both the mode boundary in the complex k_x -plane and the mode boundary in the complex ω-plane. If the wave amplitude in the coupling region is written in the form:

$$\Phi(x, t) = \phi(x, t) \exp \int ik_c(x)dx - i\omega_{0t}t, \tag{10}$$

then the partial differential equation governing the slowly varying amplitude function $\phi(x, t)$ takes the form:

$$A(x)\left[\frac{\partial^2\phi}{\partial t^2} - 2i(\frac{\partial\phi}{\partial t})s(x) - \phi s^2(x) \right] + \frac{\partial^2\phi}{\partial x^2} \tag{11}$$

$$+B(x)\left[\frac{\partial^2\phi}{\partial x\partial t} - i(\frac{\partial\phi}{\partial x})s(x) \right] + Q(x)\phi = 0$$

where:

$$A(x) = \left. \frac{\partial^2 D/\partial \omega^2}{\partial^2 D/\partial k_x^2} \right|_c, \tag{12}$$

$$B(x) = \left. \frac{-2\partial^2 D/\partial k_x \partial \omega}{\partial^2 D/\partial k_x^2} \right|_c, \tag{13}$$

$$Q(x) = \left. \frac{-2D}{\partial^2 D/\partial k_x^2} \right|_c, \tag{14}$$

and

$$s(x) = \omega_0 - \omega_c(x). \tag{15}$$

The second technique developed removes the singular behavior from the standard geometric optics hierarchy of equations in the region of a coupling point. This is accomplished through a renormalization and reordering of the hierarchy in a self-consistent manner. The resulting partial differential equation describing the slowly varying envelope function of the instability is given by:

$$A_0 \frac{\partial^2 \phi}{\partial t^2} + \frac{\partial^2 \phi}{\partial x^2} + B_0 \frac{\partial^2 \phi}{\partial x \partial t} + Q(x)\phi(x, t) = 0, \tag{16}$$

where:

$$A_0 = \left. \frac{\partial^2 D_{ii}/\partial \omega^2}{\partial^2 D_{ii}/\partial k_x^2} \right|_0, \tag{17}$$

$$B_0 = \left. \frac{-2\partial^2 D_{ii}/\partial k_x \partial \omega}{\partial^2 D_{ii}/\partial k_x^2} \right|_0, \tag{18}$$

and

$$Q(x) = \left. \frac{-2\partial D_{ii}/\partial x}{\partial^2 D_{ii}/\partial k_x^2} \right|_0 (x - x_0). \tag{19}$$

Here, D_{ij} is the element of the diagonalized dispersion tensor containing the coupling point given by Eqs. (1-3) with D replaces by D_{ij}. Note that in the near vicinity of the coupling point, $x \rightarrow x_0$, so that $s(x) \rightarrow 0$, the partial differential equation derived using the mode-boundary expansion, Eq.(11), reduces to the simpler form of Eq.(16). Although these two equations are essentially identical very near the coupling point, there are very important differences between the two results. The mode-boundary expansion, Eq.(11), is more global in nature, in the sense that it may be used to describe coupling in the presence of a group of two or more coupling points which are close together in the complex x -plane, so that a WKB description of the modes between the separate coupling points is not valid. The renormalized geometric optics expansion, Eq.(16), on the other hand, is inherently limited to the treatment of a single coupling region, which must be sufficiently separated from its nearest neighbor. By expanding the local dispersion relation along the mode boundaries in the complex k_x -plane and ω-plane, we are assured that the two modes described by our second order partial differential equation are indeed the two modes which couple at x_0. We are also able to analytically continue our equation along the mode boundaries to the physical domain of the wave propagation, the real x-axis, and are therefore certain that the partial differential equation representation is valid for real x, even though the coupling point occurs off of the real x-axis.

Using these approaches we have solved for the space-time evolution of the relativistic-electromagnetic instability[3] in an inhomogeneous magnetic field.

References

[1] G. Francis, Ph.D. Diss., Dept. of Physics, M.I.T., Cambridge, Mass., 1987.

[2] V. Fuchs, K. Ko, and A. Bers, Phys. Fluids *24*, 1261, (1981).

[3] A. Bers, J.K. Hoag, and E.A. Robertson, R.L.E. Quarterly Progress Report No. 77, April 1965, pp. 149-152.

23.4 Propagation, Mode-Conversion and Absorption in Ion-Cyclotron Heating

Analysis of energy propagation and absorption in ion-cyclotron heating of tokamak plasmas has relied on numerical solutions of fourth (and sixth) order differential equations for slab models of the plasma (poloidal) cross section. Realistic two-dimensional and fully toroidal geometry analyses would become quite unwieldy. We have undertaken to show that the analysis of the slab model can be simplified considerably. A first-order differential equation is shown to describe the transmission coefficient for the fast wave, and it is solved analytically. A second order differential equation is shown to adequately describe both transmission and reflection. Including toroidal effects in propagation, conditions for electron absorption on the mode-converted ion-Bernstein waves are also described analytically.

23.4.1 Transmission and Reflection of the Fast-Wave

The fast wave transmission coefficient can be obtained analytically using nonresonant (quasimode) perturbation theory[1] in an inhomogeneous plasma.[2] Away from the mode-conversion region, the fast wave can be described approximately by the Vlasov-Maxwell equations in the limit of $(\kappa_\perp v_T/\Omega) = 0, (v_T = \kappa T/m, \Omega = eB_0/m)$; we designate the corresponding dispersion tensor by $\overline{\overline{D}}_0$. In a large tokamak plasma, the propagation of the fast wave in these regions may be treated by the usual geometric optics formalism;[3] assuming the inhomogeneity to be in $x[\overline{B}_0 = \hat{z}B_0(x)]$, let $\overline{E}_0(x) = E_0(x)\overline{\varepsilon}_0(x)$ be the electric field, $\overline{\varepsilon}_0(x)$ its polarization vector, and $s_x(x)$ the time-averaged power flow density in x. In the localized region around mode conversion the plasma dynamics must include the effects of finite $(k_\perp v_T/\Omega)$ for ions, so that the dispersion tensor becomes $\overline{\overline{D}}_0 + \overline{\overline{X}}_1$. As regards the fast wave propagation through this region, we model it as non-resonantly perturbed by these effects to first-order in $(v_T/\Omega)^2$. Thus the perturbed fast wave electric field becomes, in general, $\overline{E} = a(x)\overline{E}_0(x)$, where $a(x)$ is a slowly-varying complex amplitude which is ordered with the nonresonant perturbation current density $\overline{J}_p = -i\omega\varepsilon_0\overline{\overline{X}}_1\cdot\overline{E}$; we then find

$$\frac{da(x)}{dx} = \frac{-\frac{1}{4}\overline{E}^*_0(x)\cdot\overline{J}_p(x, t)}{s_x(x)}, \tag{1}$$

which can be solved for $a(x)$. The power transmission coefficient is thus given by:

$$T = \frac{|\,\overline{E}(x \to -\infty)\,|^2}{|\,\overline{E}(x \to +\infty)\,|^2} = e^{-2\pi\mu} \tag{2}$$

For a plasma containing a minority ion species, e.g., hydrogen in a deuterium plasma, we find (subscripts 1 and 2 to stand for, respectively, majority (d) and minority (h) ions):

$$\mu = \frac{1}{\pi}\int_{-\infty}^{+\infty} |\,N_\perp\,|\ \mathrm{Im}\left\{\overline{\varepsilon}^*_0\cdot(\overline{\overline{D}}^a_0 + \overline{\overline{X}}_1)\cdot\overline{\varepsilon}_0\right\}d\xi = \frac{R_A}{8}\ \frac{N^5_{\perp 0}}{(1 + N^2_\parallel)^2}\left[\beta_1 + \frac{\eta}{N^2_{\perp 0}}\right] \tag{3}$$

where $\overline{\overline{D}}^a_0$ is the anti-hermitian part of $\overline{\overline{D}}_0$; $N_{\parallel,\perp} = k_{\parallel,\perp}c_A/\omega$; c_A the (majority ion) Alfven velocity; $\eta = n_2/n_1$ is the minority to majority concentration ratio; $\beta_1 = (v_{t1}/c_A)^2$ is the majority ion plasma beta $R_A = R_0\omega/c_A$; R_0 is the plasma major radius = the scale length of the (toroidal) magnetic field (B_0) variation; $= x\omega/c_A$, and $x = 0$ is the position of the majority ion's second harmonic cyclotron layer; and $N_\perp$ has been approximated by its cold-plasma value at resonance $N^2_{\perp 0} = (1 - 3N^2_\parallel)(1 + N^2_\parallel)/(1 + 3N^2_\parallel)$. The analytic result for the transmission coefficient given by (3) has been compared with numerical computations of fourth-order differential equations that model the mode conversion region.[4,5] Excellent agreement is obtained as a function of all relevant parameters, i.e., $k_\parallel$, η, n_e and T_i.

A fast wave incident upon a mode conversion region will in general undergo some reflection. Hence a more complete description of the fast wave involves describing both its transmission and reflection. This entails finding an appropriate second-order differ-

ential equation in which the coupling to the ion-Bernstein wave (i.e. mode-conversion) and dissipation (in the mode-conversion region) are incorporated in a modified propagation description of the fast wave. To obtain this we first derive an appropriately approximated dispersion relation for the fast wave from the exact hot plasma dispersion relation. Neglecting electron inertia effects and retaining terms only to first-order in $(k_\perp v_T/\Omega)^2$, we obtain the desired approximate fast wave dispersion relation.[6] Then, letting $N_\perp \rightarrow i(d/d\xi)$ we find the appropriate second-order differential equation that describes the fast wave transmission and reflection:

$$\frac{d^2F}{d\xi^2} + Q(\xi)F = 0 \tag{4}$$

where F is proportional to E_y of the fast wave,

$$Q(\xi) = \frac{(1 - 3N_\parallel^2)(1 + N_\parallel^2 - 2\Gamma_1 - 2\Gamma_2)}{1 + 3N_\parallel^2 - 3\Gamma_1 - 3\Gamma_2}\,; \tag{5}$$

$$\Gamma_1 = \frac{N_{\perp 0}^2\sqrt{\beta_1}}{4N_\parallel} Z(a_1\xi)\,;$$

$$\Gamma_2 = \frac{\eta}{4N_\parallel\sqrt{\beta_1}\,V} Z(a_2\xi)$$

$V = v_{t2}/v_{t1}$ and $v_t^2 = 2\kappa T/m$; $Z(a\xi)$ is the plasma dispersion function; $a_1 = 1/N_\parallel\sqrt{\beta_1}\,R_A$; and $a_2 = a_1/V$. The power transmission and power reflection coefficients for the fast wave can be readily obtained from numerical solutions of (4). These have been compared with results from numerical computations of fourth-order differential equations .[4,5] Excellent agreement is found for both second-harmonic and ion-ion hybrid scenarios, and as a function of $k_\parallel$ and η.

References

[1] A. Bers, In *Plasmas Physics - Les Houches 1972*, edited by C. DeWitt and J. Peyraud, New York: Gordon and Breach Science Publishers, 1975.

[2] G. Francis, Ph.D. Thesis, Dept. of Physics., M.I.T., Cambridge, Mass., 1987.

[3] H.L. Berk and D.L. Book, Phys. Fluids *12*, 649 (1969).

[4] P.L. Colestock and R.J. Kashuba, Nucl. Fusion *23*, 763 (1983).

[5] H. Romero and J. Scharer, Nucl. Fusion *27*, 363 (1987).

[6] C.N. Lashmore-Davies, G. Francis, A.K. Ram, A. Bers, and V. Fuchs, Bull. Amer. Phys. Soc. *31*, 1420 (1986).

23.4.2 Electron Absorption on the Mode-Converted Ion-Bernstein Wave

The fast wave, as discussed in sub-section 23.3.1, undergoes mode-conversion to an ion-Bernstein wave (IBW) near the second harmonic resonance layer (for a single ion-species plasma) or near the hybrid resonance layer (for a two ion-species plasma). This conversion process is efficient for small $k_{\|}$'s which carry substantial power from a single loop antenna. We have developed a numerical code which solves for the propagation of the IBW in three-dimensional torroidal geometry.[1,2] The local dispersion function, D, used for the rays is that for a hot Maxwellian plasma and includes all the nine elements of the dielectric tensor. The spatial profiles of the magnetic field, density and temperature are explicitly included in D. The toroidal ray equations have been set up for an axisymmetric tokamak with concentric flux surfaces but can be generalized to other flux surfaces. The numerical analysis shows that the IBW with small initial $k_{\|}$ propagates radially (immediately after mode conversion) away from the mode-conversion region. Along this path the poloidal mode number increases substantially. Consequently, $k_{\|}$ also increases to the point where the IBW can effectively damp on the electrons. Results show that there is a large enough increase in $k_{\|}$ for short distances (compared to the minor radius) of radial propagation that the IBW will damp its energy onto the electrons. This could help explain the experimentally observed electron heating in the ICRF heating of tokamak plasmas, as, for example, on JET.

A simple analytical model has also been developed to go along with the detailed numerical analysis. This model incorporates the essential physics of the IBW and is simple enough to provide substantial information on the propagation of IBW. Furthermore, the results from this model are in excellent agreement with the numerical results. One consequence of the model is an expression which relates the increase in the poloidal mode number, m, to the radial distance of propagation of the IBW.

$$\Delta m \approx \frac{2}{3}\frac{\omega_{cd}^2}{k_r v_{td}^2}\left(2 + 11\,\frac{v_{td}^2}{c^2}\frac{\omega_{pd}^2}{\omega_{cd}^2}\right)\frac{r\sin\theta}{R + r\cos\theta}\,\Delta r \qquad (1)$$

This result is for a deuterium plasma with a hydrogen minority. ω_{cd}, ω_{pd} and v_{td} are the deuterium cyclotron frequency, plasma frequency and thermal velocity respectively, at the radial position r (determined from the toroidal axis) where the IBW is assumed to start propagating, c is the speed of light, θ is the poloidal angle, R is the major radius and k_r is the radial wave number at the position r . The connection between $k_{\|}$ and m is given by:

$$k_{\|} = \frac{1}{|B|}\left[\left(\frac{m}{r}\right)B_\theta + \left(\frac{n}{R + r\cos\theta}\right)B_\phi\right] \qquad (2)$$

where n is the toroidal mode number, B_θ and B_ϕ are the poloidal and toroidal components, respectively, of the total magnetic field, $|B|$. Since we assume that there are no variations along the toroidal direction, n is a conserved quantity along the IBW. Consequently, an increase in $k_{\|}$ is directly connected to an increase in m. Furthermore, if

we ignore B_θ there would be no change in $k_\parallel$. Thus, the enhancement of $k_\parallel$ depends upon the presence of a poloidal magnetic field and its variation due toroidicity.

References

[1] A.K. Ram and A. Bers, Book of Abstracts, 1986 Sherwood Controlled Fusion Theory Conference, New York, Apirl 14-16, 1986.

[2] A.K. Ram and A. Bers, Bull. Am. Phys. Soc. *31*, 1420 (1986)

23.5 Relativistic Treatment of Lower Hybrid Current Drive with Wide Spectra

In hot plasmas ($T_{bulk}>1keV$) electrons resonant with lower hybrid spectra of interest to current drive have relativistic energies, and are therefore appropriately described by the relativistic Fokker-Planck equation (in momentum rather than velocity space). Previous discussions[1,2,3] of relativistic current drive have limited themselves to point or narrow-band spectra and give the corresponding figure of merit J/P_d. We have initiated a numerical and analytic study of the effect of wide-band spectra in $(p_\parallel, p_\perp)$ momentum space.[4] Results in terms of J and P_d are given for a number of situations of interest but also more detailed momentum-space behavior is discussed. Of particular interest for wide spectra is the problem of perpendicular broadening of the distribution. An analytic estimate of $T_\perp$ is found, and this permits the formulation of a theory based upon an averaged Fokker-Planck equation.

Suprathermal electrons populating the quasilinear plateau on the distribution function produced during lower hybrid current drive in hot plasmas (i.e., for bulk plasma temperatures exceeding about 1 keV) are very energetic (typically having energies up to about 1 MeV), and must be described by the relativistic Fokker-Planck equation in momentum space:

$$\frac{\partial f}{\partial t} + div(\vec{S}_{coll} + \vec{S}_{rf}) = 0 \tag{1}$$

The collisional flux vector $\vec{S}_{coll}$ is approximated to describe test electrons colliding with Maxwellian background ions and electrons. Its appropriate relativistic form is derived in Refs. 2, 3, and 5. The quaslinear flux due to RF fields $\vec{S}_{rf}$, which for lower-hybrid waves is in the parallel (to the external magnetic field) direction, is

$$\vec{S}_{rf} = \hat{p}_\parallel D_{QL} \frac{\partial f}{\partial p_\parallel} \tag{2}$$

The wave-spectrum is represented by the quasilinear diffusion coefficient D_{QL}, which was modelled by the function:

$$D_{QL} = const>0; \quad v_1 \leq v_\parallel \leq v_2 \tag{3}$$

$$D_{QL} = 0 \textit{ elsewhere}$$

The F.-P. equation (1) was solved numerically using the finite-element boundary-value-problem solver TWODEPEP supplied by IMSL. We developed appropriate pre-processor and diagnostics packages to adapt TWODEPEP for the Fokker-Planck problem. The code is currently installed on an IBM 3084, which allows the use of only up to 6 Mbytes of in-core memory. This limits our calculations to electron tails not exceeding about 800 keV, which is insufficient for bulk plasmas hotter than 1 keV, with lower-hybrid spectra whose range exceeds $v_{\parallel} = 16 v_{th}$. Nevertheless, even with these restrictions, relativistic calculations produced major differences from a non-relativistic treatment as is demonstrated in Table I.

Our focus was to carefully analyze the effect of spectrum width on the current J, and power dissipated P_d . The calculations revealed a very important effect of perpendicular broadening of the distribution function. Unlike in the nonrelativistic case, an enhanced $T_{\perp}$, here also enhances the quasilinear plateau length in $p_{\parallel}$ and hence the current. This important effect then led us to develop an analytic theory of $T_{\perp}$, so we could predict the perpendicular broadening, and this in turn enabled us to perform perpendicular averaging of the two-dimensional Fokker-Planck equation (1).

The principal problems we are now facing in the development of an appropriate one-dimensional relativistic F.-P. equation which accounts for two-dimensional dynamics are:

- relativistic coupling of $p_{\perp}$ and $p_{\parallel}$ in an ansatz for $f(p_{\perp},p_{\parallel})$.

- matching of the quasilinear plateau to the bulk of the distribution function.

The one-dimensional representation, together with two-dimensional techniques extended to include highly relativistic electrons, will enable us to study a number of questions related to LH current drive in hot plasmas.

References

[1] N.J. Fisch, Phys. Rev. A *24*, 3245 (1981).

[2] K. Hizanidis and A. Bers, Phys. Fluids *27*, 2671 (1984).

[3] C.F.F. Karney and N.J. Fisch, Phys. Fluids *28*, 116 (1985).

[4] V. Fuchs, M.M. Shoucri, C.N. Lashmore-Davies and A. Bers, Bull. Am. Phys. Soc. *31*, 1423 (1986).

[5] J.D. Mosher, Phys. Fluids *18*, 846 (1975).

Table 1

2-D Relativistic Code Results

$$T_{bulk} = 1keV; v_1 = 4v_T; D_{QL} = 3(mv_T)^2 v_o,\ v_o = 4\pi\left(\frac{e^2}{4\pi\varepsilon_o}\right)^2 \frac{\ln \Lambda n_e}{m_e^2 v_T^3},\ v_T^2 = kT/m_e$$

	Nonrelativistic			Relativistic				
v_2	Z_i	$10^2 J$	$10^4 p_d$	J/P_d	$10^2 J$	$10^4 p_d$	J/P_d	P_{max}
8	1	0.7	2.4	29	.79	2.48	32	40
12	1	2.3	4.3	53	3.2	5.3	60	40
16	1	4.8	6.3	77	14.5	12.3	118	60
16	4	7.3	13.4	55	28.3	32	88	60
16	9	9.2	27	34	44.0	74	60	60

J in units of (nev_T)

P_d in units of $(mnv_0 v_T^{\ 2})$

Note: P_{max} is the upper limit of integration in momentum, in units of (mv_T)

23.6 Absolute Instabilities from Cusp-Maps in the Complex Frequency Plane

The distinction between absolute and convective instabilities for a spatially homogeneous medium can be made by studying the dispersion relation $D(\omega,k) = 0$ of the medium, where ω is the complex frequency, and k the complex wavenumber. Let $G(x,t)$ be the response of the medium at a location x and time t to an impulsive excitation applied at the origin. The response $G(x,t)$ is expressed by the Fourier-Laplace integral:

$$G(x,t) = \frac{1}{(2\pi)^2} \int_L d\omega \int_F dk \, \frac{e^{i(kx-\omega t)}}{D(\omega,k)} \tag{1}$$

where L and F are appropriate integration contours in the complex ω and k planes, respectively. For most physical problems, the double integral in (1) cannot be easily evaluated for all t. In order to distinguish between absolute and convective instabilities, however, we only need to know the asymptotic behaviour of $G(x,t)$ for large times. This can be determined using a well-known method of analytic continuation, in which the Laplace contour L is deformed towards the lower half of the complex ω -plane. If L can be deformed below the real ω-axis, the instability is convective. Otherwise, $G(x,t \to \infty)$ is dominated by the "pinch-point" singularity having the largest temporal growth rate;[1] this is the case of an absolute instability.

The procedure described above, requires obtaining from the dispersion relation the wavenumber k as a function of the frequency ω. However, in many physical problems it is easier to determine ω as a function of k, than the other way around. For such cases, we have developed a procedure which locates pinch-points without having to map from the ω -plane into the k-plane.[2,3] This new procedure is implemented by deforming the F-contour off the real k-axis in such a way that its image in the ω-plane progresses downward from the highest branch of the map of the real k-axis (Figure 23.1). Double roots of the dispersion relation (ω_o,k_o) , are easily detected by the local angle-doubling property of the map: $(\omega - \omega_0) \sim (k - k_o)^2$. In the simplest cases, absolute instabilities occur when the deformed F -contour maps into the complex ω -plane as shown in Figure 1, where the point ω_o is found to lie in the upper-half ω-plane, beneath a single unstable branch of the image of the real k-axis. The point ω_o, connecting two Riemann sheets of the multi-sheeted ω-plane, is only covered by the image of the real k-axis on one of these two sheets. Thus, if the L-contour, deformed to pass through ω_o, is mapped in to the k-plane, its image will pinch the deformed F-contour at k_0 Consideration of this simple topology was useful in stability analysis of flow in the wake of a circular cylinder, where vortex formation was found to correspond with the absolute versus convective properties of the instability.[4] The procedure for cases leading to mappings of higher topological complexity can be found in reference [3].

References

[1] A. Bers, In *Handbook of Plasma Physics*, Vol. 1, edited by M. N.Rosenbluth and R. Z. Sagdeev, North Holland, 1983, Chapter 3.2.

[2] K. Kupfer, A. Bers, A.K. Ram, Bull. Am. Phys. Soc. *31*, 1402 (1986).

[3] K. Kupfer, A. Bers, and A.K. Ram, M.I.T. Report PFC/JA-87-13 (1987); to appear in Phys. Fluids 1987.

[4] G.S. Triantafyllou, M.S. Triantafyllou, C. Chryssostomidis, J. Fluid Mech. *170*, 461 (1986).

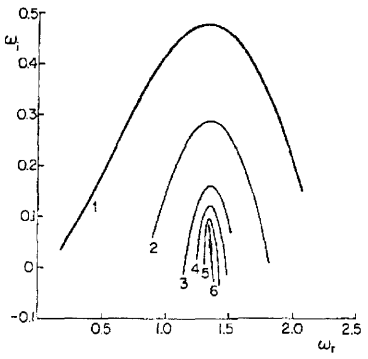

Figure 23.1. : Curve 1 image of the real k-axis in the ω plane; curves 2 through 6: images of lines parallel to the real-k axis. The pinch point is located at the cusp of curve 6.

23.7 Physics of Thermonuclear Plasmas

U.S. Department of Energy (Contract DE-AC02-78ET-51013)

Bruno Coppi

The main theme of this program is the theoretical study of plasmas in thermonuclear regimes. Topics include, but are not limited to, study of basic plasma properties (stability, transport, ...), simulation of present day and future experiments on magnetically confined plasmas, and design of machines for fusion burn experiments and advanced fuels. Theoretical guidance for and participation in the Alcator experimental program are an important part of our effort.

We are particularly interested in the physics of high density plasmas that has been pioneered by the Alcator program in view of its outstanding confinement as demonstrated by the record values of the parameter, $n\tau_E$, and the degree of plasma purity $1/(Z_{eff}-1)$ achieved. An analysis that we presented to the Department of Energy about six years ago indicated that shorter than expected confinement times in Alcator C plasmas should have been attributed not to a degradation of electron energy confined but instead to an increase of the ion thermal conductivity. This analysis led to the well known pellet injection experiments in Alcator C that result in the record $n\tau_E$. The circumstantial evidence for our analysis was an observation that density profiles formed as a result of neutral gas injection in Alcator C were "flatter" than those of other experiments. In particular, the parameter:

$$\eta_i = \frac{d\ell n T_i}{dr} \Big/ \frac{d\ell n n}{dr}$$

had values, even in the central part of the plasma column, that were above the threshold for the onset of "ion mixing modes" that can produce a strong effective ion thermal conductivity. Therefore, it was natural to suggest that the "cure" was to be found in producing density profiles that were peaked to the extent that η_i could be close to unity and the relevant experiments appear to have confirmed our expectation. In fact, the idea of "profile consistency" that was being formulated at that time implied that it would have been difficult to alter the canonical shape of the electron temperature profile, compared to the relative ease with which density profiles were modified. The concomitant prediction that the impurity transport had to be influenced by the change in η_i been also verified by the observations. These circumstances and the need to have a firmer basis, than presently available, on which to predict the ion thermal energy losses in future ignition experiments, have led us to intensify our efforts and those of our colleagues at the Princeton Plasma Physics Laboratory on developing further the linear and the nonlinear theory of ion mixing modes. At the same time, we have started an effective collaborative effort with our colleagues of the (Princeton) TFTR team who have carried out the latest pellet injection experiments. These experiments, performed for the purpose of providing (if possible) a detailed interpretation of energy losses, have achieved new record values of the confinement parameter $n\tau_E$.

The line of compact experiments that we have proposed first in 1975, as a follow up to the Alcator and Frascati Torus programs, and developed through a series of design studies in later years was adopted as the next major undertaking of the U.S. fusion program in 1985; three major centers (Lawrence Livermore National Laboratory, M.I.T., and Princeton) are now committed to this line of investigation. In addition, following the agreements to pursue collaboration in fusion research with the U.S.S.R. concluded at the Geneva Summit meeting, a compact ignition experiment has been considered as the first step to be taken in a more general frame for the development of fusion research through the end of this century. Meanwhile, the Ignitor effort that was initiated in Europe about 10 years ago has been stepped up and a set of tests on the most critical machine component is being planned.

The Alcator C-Mod machine that is now under construction at M.I.T. is based on a magnetic confinement configuration adopted already in the Ignitor design and that we had studied in the early seventies under the name of Megator. Those studies proposed experiment that, like Alcator C-Mod, combine high magnetic field and compact geometry with tight aspect ratio and elongated plasma cross section. Such designs were intended to produce plasma currents exceeding 1 Mega Amperes while maintaining current densities in the same range as those expected, at that time, in the Alcator experiments.

In the next subsections we present several major topics of theoretical investigation: the principle of profile consistency, fishbone oscillations in beam injected as well as ignited tokamaks, transport simulations in current and planned experiments, and an analysis of the pathways to ignition.

23.7.1 Profile Consistency

Among the general criteria that we have tried to formulate a few years ago in order to describe the "anomalous" transport characteristics (that are not explained by clas-

sical transport theories that include the effects of discrete particle collisions only) of magnetically confined plasmas is the so-called "Principle of Profile Consistency." [1] The main implication of this principle is that the transport coefficients that conform to it depend on the global properties of the plasma column. Another implication is that there are two kinds of physical processes involved: one that reconstructs the canonical electron temperature profile after it is severely disrupted, such as when a massive pellet is injected in the plasma column, and one that determines the rate of electron energy transport under nearly steady state conditions. Thus a variety of transport equations that can describe both processes have been considered, including one that involves the presence of an inward flow term that is difficult to justify on the basis of the properties of known microinstabilities and is not suitable to represent the wider range of experimental information now available. Instead it is more appropriate to introduce an effective thermal conductivity that has a nonlinear dependence on the electron temperature gradient, such as

$$\kappa_{eff} = \left[\kappa_s^2 + \kappa_F^2 \left(\frac{a^2}{T_e \dot{\alpha}} \quad \frac{\partial T_e}{\partial r^2} + 1 \right)^2 \right]^{1/2},$$

where the canonical electron temperature profile is represented by $T_e^c(r) = T_{eo} \exp(-\alpha)$, $\alpha \equiv \alpha(r^2/a^2)$, a is the plasma minor radius, κ_s is the thermal conductivity that persists when T_e is completely relaxed on the $T_e^c(r)$ profile, and κ_F the coefficient corresponding to the fast process that rearranges $T_e(r)$ when it is forced to depart from $T_e^c(r)$. Considering $\kappa_F^2 > \kappa_s^2$ and steady state conditions, the peak value T_{eo} is determined by the "minimum departure condition," namely that

$$F(T_{eo}) = \int_0^{\alpha_b} \frac{d\alpha}{\kappa_f} \left[\left(\frac{\bar{S}_e a^2}{4\dot{\alpha} T_e^c} \right)^2 - \kappa_s^2 \right]^{1/2}$$

be a minimum; α_b denotes the value of α at the edge of α the plasma column where $\bar{S}_e(r) \equiv (2/r^2) \int r' S_e(r') dr'$, $S_e(r)$ is the electron energy source and $\alpha_b \equiv \alpha(r = a)$. Therefore κ_s need not be function of the profile of $S_e(r)$ in order to enforce profile consistency and can be used directly as derived from a nonlinear theory of the type of microinstability deemed to be responsible for it. One that is considered of special interest for this is the so-called ubiquitous mode[2] that is driven by the electron temperature gradient and produces thermal energy transport without corresponding particle transport. In the case where only ohmic heating is present, the adopted diffusion coefficient $D_{th}^e = \kappa_s/n$ is

$$D_{th}^e \simeq 2.4 \times 10^{18} (a/r) B_\theta / (n T_e) (Z./A_i)^{1/4} (q_s R)^{-1/2} cm^2/\ sec$$

where T_e is in keV, B_θ in kG, n in cm^{-3}, R in cm, $Z./A_i \equiv v_s^2/(T_e/m_p)$, m_p the proton mass and v_s the ion sound velocity of the considered plasma. When injected heating is dominant

$$8\pi/(B_\theta r)^2 \int_o^r dr^2 \ \ d(nT_e)/d\ell nr$$

becomes the limiting factor and D_{th}^e acquires the scaling $D_{th}^e \propto 1/B_\theta$. The existence of two processes, fast and slow, on the temperature evolution has been confirmed by the Alcator pellet injection experiments.[3] Observations made by electron cyclotron emission have shown that, within a time of the order of 200 μsec-300 μsec after the central

electron temperature has dropped due to the injection of the pellet, the electron temperature profile recovers its typical Gaussian shape. This time scale is shorter by as much as two orders of magnitude than the electron energy transport time scale controlled by κ_s The propagation of sawtooth heat pulses is also indicative of the existence of two transport time scales.

23.7.2 Fishbones

The most striking of all collective processes that have been so far observed in magnetically confined, neutral beam-injected plasmas is the so-called "fishbone instability," named after the characteristic skeletal signatures of the plasma temperature and poloidal magnetic field fluctuations.[4–8] Fishbone bursts are correlated with losses of energetic beam particles, reducing the beam heating efficiency and thus limiting the maximum achievable β (=kinetic pressure/magnetic pressure). The mode structure is typically dominated by the $m^\circ = 1$, $n^\circ = 1$ poloidal and toroidal harmonics, with a frequency of oscillation in the 10-20 kHz range. This frequency is of the same order and sign[9] as that of both the core-ion diamagnetic frequency ω_{di} and the magnetic drift frequency ω_{Dh} of energetic beam particles that are trapped in magnetic wells along the equilibrium field lines. The appearance of fishbone activity coincides roughly with the threshold for the onset of pressure-driven $m^\circ = 1$ internal kink modes in a toroidal confinement configuration.

We have proposed[10,11] a theoretical model of the linear instability process based on the following: 1) the excited mode has a frequency of oscillation nearly equal to the ion diamagnetic frequency and is one of the two $m^\circ = 1$ modes that are found under the conditions for ideal MHD instability, but are rendered marginally stable by finite ion Larmor radius effects of the core-plasma; 2) the mode excitation energy is related to the plasma pressure gradient; and 3) the presence of a "viscous" dissipative process, e.g., produced by a mode-particle resonance, is required for this instability to develop. In the case of perpendicular netural beam injection, the relevant mode particle resonance is $\omega = \omega_{Dh}^{(o)}(\varepsilon, \mu)$, where $\omega_{Dh}^{(o)}$ is the average-along-the-orbit magnetic drift frequency of energetic ions having energy $\varepsilon = (1/2)m_h v^2$ and magnetic moment $\mu = (1/2B)m_h v_\perp^2$. In fact, $\omega_{di}/\omega_{Dh}^{(o)} \sim (T_i/T_h)(R/r_n) \times (1 + \eta_i) \sim 1$ for typical beam parameters, where $T_{i(h)}$ is the core-ion (hot-ion) temperature, $r_n = |d\ell n n_i/dr|^{-1}$ and $\eta_i = d\ell n T_i/d\ell n n_i$.

As a consequence of the excited mode, resonant beam ions can be transported out of the plasma column.[12,13] In Ref. 10 we have constructed a simple nonlinear model for the instability cycle based on the resistive damping of the fishbone mode once the number of resonating particles has dropped sufficiently. Another possibility is that the saturated mode may be damped in a process connected to the spatial phase mixing of an Alfven wave packet, as was first proposed in Ref. 14.

These considerations lead to the following picture for the interplay between fishbone bursts and sawtooth oscillations. The instabilities of the fishbone mode and the resistive internal kink mode involve different threshold values of the poloidal beta, $\beta_p = [8\pi/B_\theta^2(r_o)][\bar{p}(r_o) - p(r_o)]$, where $\bar{p}(r_o) = r_0^{-2}\int^{r_o} p(r)dr^2$ and r_o is the radius of the mode rational surface where the inverse rotational transform $q=1$. For the resistive kink, $\beta_{p,crit}^{rk}$ is determined by the combined effects of ion viscosity and ion diamagnetic frequency.[15] Since the resistive kink mode has a frequency much lower than ω_{di} it does not interact efficiently with the beam and thus depends on resistivity for the dissipation. The threshold

value for the fishbone mode is lower, $\beta_{p,crit}^{fm} < \beta_{p,crit}^{rk}$. The value of β_p increases along the sawtooth ramp, as the pressure profile steepens. When, $\beta_{p,crit}^{fm} < \beta_p < \beta_{p,crit}^{rk}$, only the fishbone mode is unstable, but it saturates and decays quickly on a fast (a few msec) time scale, resulting in expulsion of energetic particles while leaving the macroscopic central plasma region essentially unaffected. As soon as β_p exceeds $\beta_{p,crit}^{rk}$, the resistive internal kink mode is excited and it determines the "crash" of the sawtooth.

We emphasize that this physical picture relies on the assumption of relatively large values of the core-ion diamagnetic frequency. When diamagnetic frequency effects are neglected, a recent analysis,[16] valid for arbitrary values of the ideal MHD energy functional, has determined that ion viscosity brings about a reduction in the growth rate of the $m^\circ = 1$ mode, but by itself is insufficient to completely stabilize it. When the core-ion diamagnetic frequency is large, on the other hand, ion viscosity stablization is easily achieved.[15]

These results have several consequences for the prediction of sawtooth oscillations in compact ignition experiments,[17] to the extent that the plasma can be driven near (or past) the ideal MHD marginal stability threshold of $m^\circ = 1$ modes. First, sawtooth crashes may occur only when the minimum value of δW exceeds a (possibly negative) threshold value during the temperature ramp, as the pressure profile steepens. Second, sawteeth may be suppressed even though $q<1$ in part of the plasma. Third, in toroidal plasmas where the "poloidal beta" parameter is relatively high and the $m^\circ = 1$ instability is driven primarily by the pressure gradient, disruptions may relax the pressure profile only, leaving the q-profile unchanged.

23.7.3 Transport Simulation

The investigation of the radial energy balance and thermal transport in large size Ohmic plasmas carried out in collaboration with Princeton Plasma Physics Laboratory has reached a major milestone, where a one dimensional, numerical transport model with sawtooth oscillations has been shown[18,19] to reproduce Ohmic TFTR plasmas run from 1983-86. Some 40 representative discharges were simulated, including current, density, and toroidal magnetic field scans from different operating periods. The numerical model can be used to characterize a "standard" TFTR Ohmic discharge (without anomalous ion thermal conductivity). It provides a sensitive check on Z_{eff} and, to a lesser extent, plasma composition measurements beyond that available from a standard analysis code. Points of discrepancy between simulation and experiment have been analyzed and accounted for.

Analysis of the simulated discharges shows the inherent limitations on the accuracy to which a transport model can be determined from experiment under fairly ideal conditions (well-diagnosed plasma, similar types of discharges). The extent to which a different driving mechanism can be supported by experiment has been investigated by considering ranges of parameters, including varying size plasmas.[19,20] Assuming the fundamental nature of profile consistency (for either the electron temperature T_e or the toroidal current density J_ϕ), the major effect of a different driving mechanism is to change the dependences of voltages, peak temperatures, and energy confinement times on the plasma parameters. Rather than model different diffusion coefficients, the original transport results were analyzed for trends in the discrepancy between simulation

and experiment. Results suggest a stronger inverse dependence of the diffusion coefficient on the major radius R, indicative of gradient-driven or drift wave type transport. However, the results are not conclusive because of the accumulated differences due to the experimental uncertainties and to the systematic variations between different types of discharges, which have not been quantified before. Trials with different diffusion coefficients also show that the dependence on the plasma parameters is difficult to distinguish, as long as a reasonable temperature profile shape is produced. The likely thermal transport mechanisms are thus difficult to distinguish on the basis of Ohmic data alone. Auxiliary heating adds other uncertainties, as well as changing the underlying plasma instabilities when it is strong.

Sawtooth oscillations, in the model used, were shown to have relatively little ($\sim$ 10%) effect on the volume integrated energy balance, despite large changes in the electron temperature (30% in T_{eo}), toroidal current density, and Ohmic heating radial profiles.[20] The effect was studied by disabling the trigger for the sawtooth crash, while retaining the best fit input parameters and thus shows the effect of the numerical model. Flattening the temperatures and particle densities during an instantaneous crash, and redistributing the current according to helical flux conservation adequately accounts for the roughly linear variation of $T_{eo}/<T_e>$ (central/volume average) with the safety factor q_a at the plasma edge. Experimental profiles (ECE) indicate an additional narrowing of the T_e profile with increasing q_a noticeable at higher $q_a \geq 4$.

In the past year we have added alongside the relatively simple, fast one dimensional transport code a more complex 1 1/2 D version (BALDUR, modified by Glenn Bateman of Princeton Plasma Physics Laboratory). Thus we have been able to self-consistently take into account effects important for compact ignition experiments, such as the paramagnetic increase in the magnetic field at low β_p, the distribution of plasma current with a realistic geometry, the time dependent evolution of the plasma configuration due to the initial ramping of current and magnetic field.[21] Using similar transport models, results from this code generally confirm our earlier predicitons of the behavior of the ignition process.[17,22] As expected, some vary, for instance, the sawtooth size increases in 1 1/2 D with a helical flux conservation model.

We are using the 1 1/2 D code in collaboration with our other research efforts to model new Ignitor parameters, test the effects of different forms for anomalous electron thermal transport, and investigate the consequences for ignition of the possible presence of anomalous ion heat transport due to η_i modes.[23] Since the latter transport increases strongly with T_i its effects can be quite deleterious if it extends over a significant portion of the plasma column.

An extension to DD and D^3He fusion regimes has been under way for the 1D code and is planned for the 1 1/2 one as well. It incorporates the set of fusion reactions between D, T, He^3 and their fusion products in a self-consistent manner, keeping track of fusion "ash" as well as energetic particles. The macroscopic effects of synchrotron radiation will be included. The ignition scenario envisions DT ignition with auxiliary heating in a modified compact ignition device, then addition of D and He^3. Initial studies have been done of the device parameters with DT alone.

23.7.4 Density Limit and Path to Ignition

In order to reach ignition, it is desirable to maintain the highest possible value of the confinement parameter $n\tau_e$, implying operation at relatively high densities where collisional (neoclassical) ion thermal losses and electron-ion bremsstrahlung become significant in the global energy balance. These losses are equal to the energy per unit time deposited by the fusion reaction products at the "minimum ignition temperature." Near and above this temperature, the presence of anomalous ion thermal conductivity due to collective modes can strongly affect the optimal value of the density that yields the fastest approach to the attainment of ignition for a given amount of external power. We have considered in particular the so-called η_i modes[23] with perpendicular wavelengths considerably greater than the ion gyroradius, which produce an ion thermal conductivity proportional to $nT_i^{3/2}$. In collaboration with W. Tang of Princeton Plasma Physics Laboratory, we have constructed an approximate model equation for the steady state energy balance in the central region of the plasma column and have obtained multi-valued solutions for the density as a function of temperature, ion thermal anomaly strength, and external heating power.[24]

For the case of no ion anomaly, there is a maximum density allowed for the plasma to reach the minimum ignition temperature T_m, while beyond T_m all densities are allowed. In the presence of an anomaly, a critical external power must be supplied to provide a channel between allowed density regions as the temperature increases beyond T_m. For a realistic temperature dependence of the fusion reaction cross section, the density must be progressively adjusted above a minimal value in order to heat the plasma to temperatures considerably larger than T_m.

We have verified the analytical properties of the model equation with 1 1/2 D numerical simulations,[17,25] applied to the parameters of the Ignitor compact ignition experiment.

References

[1] B. Coppi, Comments Plasma Phys. Controlled Fusion *5*, 261 (1980).

[2] B. Coppi and G. Rewoldt, Phys. Rev. Lett. *33*, 1320 (1974).

[3] C.C. Gomez, Ph.D. Diss., M.I.T., Cambridge, Mass., Report PFC/RR-86-8, 1986.

[4] K. McGuire et al., Phys. Rev. Lett. *50*, 891 (1983).

[5] D. Johnson et al., In *Plasma Physics and Controlled Fusion Research*, Vienna: I.A.E.A., 1983, Vol. 1, p. 9.

[6] J.D. Strachan et al., Nuclear Fusion *25*, 863 (1985).

[7] D.O. Overskei et al., In *Heating in Toroidal Plasmas*, Rome: E.N.E.A., 1984, Vol. 1, p. 29.

[8] W.W. Heidbrink et al., Phys. Rev. Lett. *57*, 835 (1986).

[9] B. Coppi, contribution presented at the Varenna Workshop on Plasma Transport, Varenna, Italy, 1982, and at the PPPL Workshop on Bean-Shaped and High-β Tokamaks, Princeton, New Jersey, 1983.

[10] B. Coppi and F. Porcelli, Phys. Rev. Lett. *57*, 2272 (1986).

[11] B. Coppi, S. Migliuolo, and F. Porcelli, submitted to Phys. Fluids (1987).

[12] B. Coppi and A. Taroni, Plasma Phys. *26*, 2958 (1983).

[13] R.B. White et al., Phys. Fluids *26*, 2958 (1983).

[14] V.W. Gribkov, B.B. Kadomtsev and O.P. Pogutse, JETP Lett. *38*, 15 (1983).

[15] F. Porcelli and S. Migliuolo, Phys. Fluids *29*, 1741 (1986).

[16] F. Porcelli, Phys. of Fluids *30*, 1736 (1987).

[17] B. Coppi, R. Englade, S. Migliuolo, F. Porcelli, and L. Sugiyama, in *Plasma Physics and Controlled Nuclear Fusion Research*, Kyoto, Japan (to be published by I.A.E.A., Vienna, 1987).

[18] J. Martinell, Ph.D. Thesis, Dept. of Physics, M.I.T., Cambridge, Mass., 1986.

[19] L. Sugiyama, J. Martinell, and P. C. Efthimion, "Predictive Transport Simulation of TFTR Ohmic Discharges," M.I.T., R.L.E. Report PTP-87/1, submitted to Nucl. Fusion.

[20] L. Sugiyama, "R and a Dependence of Electron Anomalous Thermal Transport," M.I.T., R.L.E. Report PTP-86/8, August 1986.

[21] R. Englade and L. Sugiyama, *Sherwood Theory Conference*, New York, 1986.

[22] L. Sugiyama, M.I.T., R.L.E. Report PTP-84/2, 1984.

[23] T. M. Antonsen, Jr., B. Coppi and R.C. Englade, Nuclear Fusion *19*, 641 (1979).

[24] B. Coppi and W. Tang, Princeton Plasma Physics Laboratory Report PPPL-2343, 1986, submitted to Phys. Fluids.

[25] R. Englade, Bull. Am. Phys. Soc. *31*, 1565 (1986).